

RESEARCH ON DYNAMIC INTERACTIONS BETWEEN THE PIPE AND CORAL FOUNDATION OF THE SPRATLYS ISLANDS

NGUYEN VIET DUC

Industrial University of Ho Chi Minh City, Vietnam – Email: ducnguyencsic@gmail.com

LE TAN

Industrial University of Ho Chi Minh City, Vietnam – Email: letan7012@gmail.com

(Received: September 09, 2016; Revised: October 28, 2016; Accepted: December 06, 2016)

ABSTRACT

This paper presents some results of geological construction characteristics by depth of the Southwest Cay Island's coral foundation, the Spratlys Islands, and the interaction between pipe and coral foundation under the effect of load of shockwave bombs. The problem of interaction between the pipes and coral foundation is resolved on the basis of finite element method and Matlab programming. The results could contribute to research on calculating, designing and constructing projects on the island to serve for defense of the country and livelihoods on the island.

Keywords: coral foundation; dynamic interaction; finite element method; nonlinear dynamics; slip element; substrate.

1. Introduction

Vietnam is a country with over 3,000 km long coastline, besides currently offshore islands now belonging to Vietnam maritime territory are mostly coral islands, which are distributed into several dispersed clusters. The clusters are important shields surrounding maritime territory and coastline of Vietnam, because they are responsible for defending borders of our seas and make great contribution in maintaining the security, defense and construction of the country (Nguyen, 2006). Being aware of the importance of these issues, the Government has made the right decision to build the Spratlys islands becoming a military base with a strong economy, which is capable of meeting the short- and long-term tasks. This is also shown in "Sea Strategy to 2020", which has been already adopted by the Parliament. To do this, apart from the preparation of human resources, weapons and equipment, it is inevitably necessary to research on building and restoring marine infrastructures properly,

and to find out the optimal solutions for the construction of offshore island structures.

From now on and in the future, many constructions will be built on the coral islands of the Spratly Islands, including Southwest Cay Island - one of the strategic islands in Vietnam military and civil. The data on the geological characteristics and physical properties of the coral island is limited, so it is difficult to calculate, design, execute and take advantage of defense projects and livelihoods on the island in an effective way. Thus the research on the results of the coral foundation in the Spratlys for constructing and developing the island's marine projects is an urgent issue for science nowadays (Nguyen et al., 2008). The geological data are from the positive collaboration between the author and the research team of the state-level projects (Hoang, X. L., 2005). Geological characteristics of coral substrate on Southwest Cay Island were studied on the basis of deep boreholes 51,2m done by specialist team performing the project on this island (Figure 1).

Characteristics of geological construction by depth of the Southwest Cay island's coral foundation, the Spratlys Islands

In terms of tectonics, Southwest Cay Island is made of coral branches and coral blocks. After analyzing results of survey in reality and test on samples of coral in the laboratory (Figure 2), the authors have identified geological structure of the coral's rock layers by depth of borehole following:

Layer 1: Spongy removable structure, water saturation.

Layer 2: Milky white, this layer is relatively soft.

Layer 3: Milky white, this layer is relatively firm.

Layer 4: Milky, this layer is relatively hard.

Layer 5: Slightly premature cornerstone coral, white milk, this layer is specially firm.

Layer 6: Firmly spongy coral, milky white, relatively firm.

Layer 7: Firm root coral, milky white, firm and flexible layers.

Layer 8: Firm corals with large blocks, milky white, firm and spongy.

Layer 9: Coral blocks with small and medium size, very firm.



Figure 1. Fielding and sampling on Southwest Cay island

Layer notation	Bottom layer height	Bottom layer depth	Thickness	Borehole section	Stratigraphic over
1	1.08	3.70	3.70		Yellow gravel and crushed coral branches
2		7.00	3.30		Crush coral branches
3	-14.52	19.3	12.3		Original hard corals interspersed many small local
4		23.3	4.0		Original hard corals interspersed big local
5	-21.82	26.6	3.3		Hard coral root, plastic
6	-23.82	28.6	2.0		Original hard corals interspersed many small local
7		43.3	14.7		Hard coral root, plastic
8	-40.52	45.3	2.0		Hard coral root
9	-46.42	51.2	5.9		Medium and small local

Figure 2. Profile of a borehole at the depth of 51,2m at Southwest Cay island

After analyzing experiment's data, authors have identified mechanical and physical characteristics of samples by depth of borehole as Table 1 and 2. In Table 2, the

symbol "-" stands for the absence of data samples for separation or sizes which do not guarantee the standards of samples.

Table 1

Density, Specific weight, Porosity of corals

No	Sampling Depths [m]	Density γ [g/cm ³]		Specific Weight ρ [g/cm ³]	Porosity n [%]
		Rough	Saturation		
1	11,50	1,78	2,11	2,85	34,0
2	18,00	1,87	2,08	2,80	33,2
3	18,40	2,03	-	2,81	27,8
4	20,50	2,10	2,27	2,81	25,3
5	23,00	2,03	2,25	2,79	27,2
6	24,00	1,34	1,71	2,72	50,7
7	24,40	1,75	1,99	2,71	35,4
8	24,80	1,53	1,71	2,72	43,8
9	25,60	1,70	1,901	2,72	37,5
10	25,80	1,75	1,94	2,72	35,7
11	28,60	1,73	1,96	2,70	35,9
12	29,30	1,83	2,02	2,72	32,7
13	33,00	1,96	2,03	2,70	27,4
14	34,00	2,01	2,17	2,72	26,1
15	39,70	1,97	2,13	2,69	26,8
16	40,00	1,84	1,94	2,70	31,9
17	40,30	1,94	2,11	2,70	28,1
18	43,00	2,01	2,16	2,69	25,3
19	43,90	2,11	2,21	2,71	22,1
20	49,20	2,37	2,44	2,72	12,9

Table 2

Compressive strength, softening ratio, elastic modulus, Poisson ratio

No	Sampling Depths [m]	Softening Coefficient	Durable compression strength R [N/cm ²]		Elastic modulus [$\cdot 10^5$ N/cm ²]	Poisson Ratio ν
			Rough	Saturation		
1	11,50	-	-	-	-	-
2	18,00	-	-	-	-	-
3	18,40	-	-	-	-	-
4	20,50	-	-	-	-	-

No	Sampling Depths [m]	Softening Coefficient	Durable compression strength R [N/cm ²]		Elastic modulus [·10 ⁵ N/cm ²]	Poisson Ratio ν
			Rough	Saturation		
5	23,00	-	-	-	-	-
6	24,00	0,75	278,0	208,0	0,6	0,19
7	24,40	0,75	620,0	463,0	1,38	0,22
8	24,80	0,82	427,0	351,0	1,29	0,32
9	25,60	0,94	1027,0	965,0	7,24	0,22
10	25,80	0,85	808,0	685,0	1,54	0,25
11	28,60	-	-	-	-	-
12	29,30	0,87	815,0	712,0	2,57	0,20
13	33,00	0,88	681,0	599,0	2,77	0,15
14	34,00	0,81	452,0	366,0	1,83	0,39
15	39,7	0,89	861,0	769,0	2,24	0,19
16	40,00	0,83	532,0	444,0	1,68	0,18
17	40,30	0,91	1100,0	999,0	3,85	0,21
18	43,00	0,86	834,0	719,0	2,34	0,17
19	43,90	-	-	-	-	-
20	49,20	-	-	-	-	-

Remarks

- By depth, coral foundation separates into many kinds of layers: complete and incomplete.

- By depth, there happens a huge change compared to a small change of modulus of elasticity and Poisson's ratio only has small change. The porosity of the layer is relatively large (12.9÷ 40.62) %.

- It can be asserted: coral is kind of brittle materials with stressor - linear deformation, the link between building structure and coral substrate is one-way (pressure, no tension).

2. Calculation of dynamic interaction between the pipe and coral foundation under the weight of bombs' load

This content is made on the basis of inheriting the results of research on geological construction of coral foundation that were shown above and the finite element theory.

2.1. Effects of bombs' load on construction

When the bomb exploded, the process of implementing extremely fast lateral spread response in a short time with a large amount of energy released in a limited volume of explosive blocks spreading around that affected on everything. The sudden release of energy raises the temperature and pressure and the explosive expansion makes air highly compressed forming shock waves (Zhu and Lu, 2007). Shock wave consists of 2 areas: the compression phase and the relaxation phase (Figure 3).

Since compression pressure is many times as huge as relaxation pressure. Therefore in reality we use compression pressure to make calculations, and then the load function is shown in Figure 3.

$$\Delta p(t) = \Delta p_{\phi} \left(1 - \frac{t}{\tau} \right) \quad (1)$$

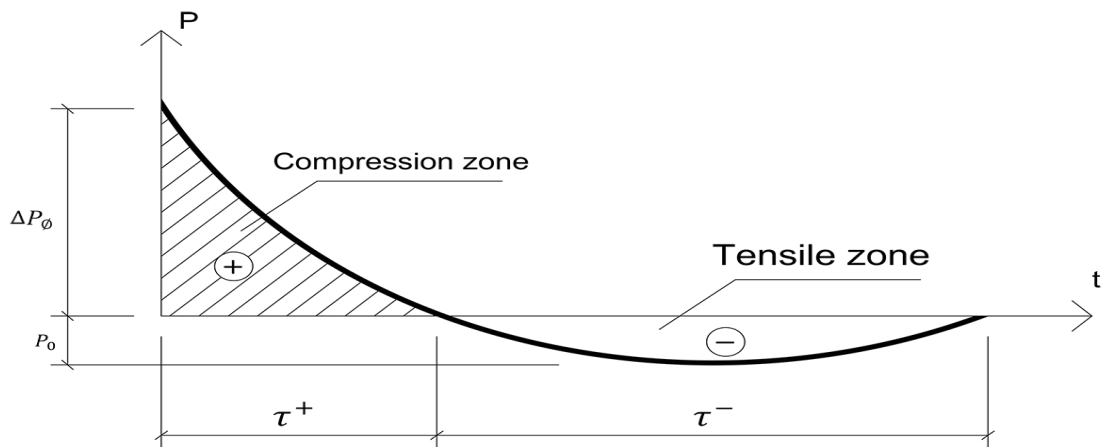


Figure 3. Shockwaves diagram

2.2. Finite element algorithms to solve problems

The authors solved similar problem by following plane strain model, in the view of processing the pipes and the coral substrate at the same time under the finite element method - FEM (Bath and Wilson, 1982, Zienkiewicz and

Taylor, 1986), in which used a combination of the 4 - node quadrilateral plane deformation element (pipes and the substrate near the pipe), 3 - node triangular element (the substrate distant the pipe) and the 4 - node contacting elements (PTTX) (between the platform and the pipe). FEM model is shown in Figure 4.

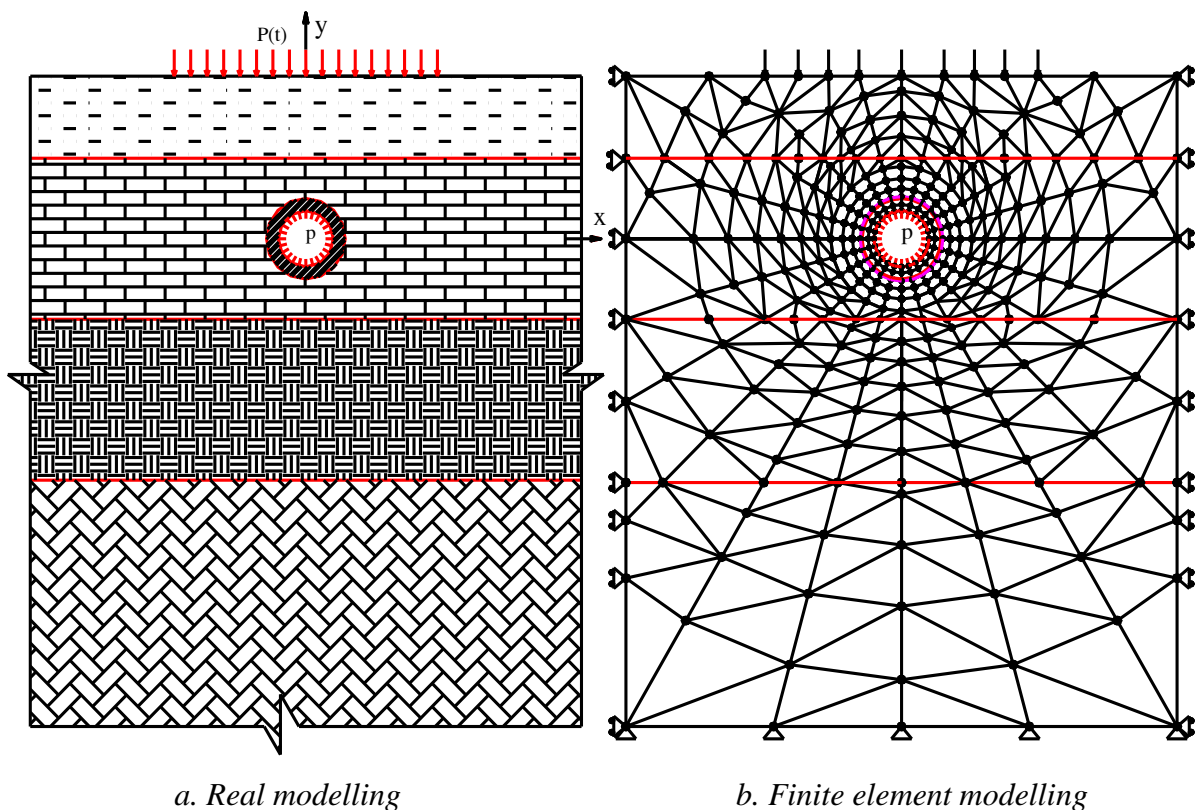


Figure 4. Modelling of the structure

The assumptions for calculating in this paper are based on the results from the work included in the literature elsewhere [Hoang, X. L., 2005; Nguyen T. C., 2006] as follows:

1) The pipe material is elastic, linear distortion; coral foundation is layering, each layer of material is homogeneous, isotropic, linear distortion;

2) The pipe and coral foundation are working under plane strain condition. The relationship between the pipe and coral foundation is one-way links through intermediary elements – contact elements (Amir Rahim, 1998);

3) No separate phenomena, sliding among the foundations.

Under the effect of loads shockwave, the equation of structural dynamics, presented before elsewhere [Bath and Wilson, 1982; Zienkiewicz and Taylor, 1986], can be expressed as:

$$[M]\{\ddot{U}\} + [C]\{\dot{U}\} + [K]\{U\} = \{R(t)\} \quad (2)$$

Where: $[M]$ is the mass matrix, $[C]$ is the damping matrix, $[K]$ is the stiffness matrix, $\{U\}$, $\{\dot{U}\}$ and $\{\ddot{U}\}$ are displacement vectors, velocity and acceleration vectors respectively; $\{R(t)\}$ is the load vectors.

The normal stiffness k_n and shear stiffness k_s contract point depends on displacement vector $\{U\}$, so stiffness matrix also depends on displacement vector $\{U\}$: $[K_{se}] = [K_{se}(\{U\})]$. This led to the overall stiffness matrix of the system (set from the matrix element) is also dependent on displacement vector $\{U\}$:

$$[K] = \sum_e [K]_e = [K(\{U\})] \text{ and}$$

$$[C] = \alpha[M] + \beta[K] = [C(\{U\})] \quad (3)$$

Where: α and β are Rayleigh damping coefficients.

Thus (2) is non-linear equations and rewritten as:

$$[M]\{\ddot{U}\} + [C(\{U\})]\{\dot{U}\} + [K(\{U\})]\{U\} = \{R(t)\} \quad (4)$$

To solve the non-linear equation (4) the authors combined the direct integration method Newmark and Newton - Raphson iterative method on each time step Δt according to [Bath and Wilson, 1982; Zienkiewicz and Taylor, 1986].

$$[M]\{\ddot{U}_{t+\Delta t}\}^{(i)} + [C_{t+\Delta t}]^{(i-1)}\{\dot{U}_{t+\Delta t}\}^{(i)} + [K_{t+\Delta t}]^{(i-1)}\{\Delta U\} = \{R_{t+\Delta t}\} - \{P_{t+\Delta t}\}^{(i)} \quad (5)$$

$$\{\dot{U}_{t+\Delta t}\}^{(i)} = a_1(\{U_{t+\Delta t}\}^{(i-1)} + \{\Delta U\}^{(i)} - \{U_t\}) - a_4\{\dot{U}_t\} - a_5\{\ddot{U}_t\} \quad (6)$$

$$\{\ddot{U}_{t+\Delta t}\}^{(i)} = a_0(\{U_{t+\Delta t}\}^{(i-1)} + \{\Delta U\}^{(i)} - \{U_t\}) - a_2\{\dot{U}_t\} - a_3\{\ddot{U}_t\} \quad (7)$$

$$\{U_{t+\Delta t}\}^{(i)} = \{U_{t+\Delta t}\}^{(i-1)} + \{\Delta U\} \quad (8)$$

$$\text{where: } a_0 = \frac{1}{\alpha \Delta t^2}; a_1 = \frac{\delta}{\alpha \Delta t}; a_2 = \frac{1}{\alpha \Delta t};$$

$$a_3 = \frac{1}{2\alpha} - 1; a_4 = \frac{\delta}{\alpha} - 1; a_5 = \frac{\Delta t}{2} \left(\frac{\delta}{\alpha} - 2 \right);$$

In the above algorithm, δ and α are parameters that have to be complied with the constraints $\delta \geq 0.5$ and $\alpha \geq 0.25(0.5 + \delta)^2$.

Using the equations (6) and (7), the equation (5) can be rewritten as follows:

$$[K_{t+\Delta t}^*]^{(i-1)} \cdot \{U\}^{(i)} = \{R_{t+\Delta t}^*\}^{(i-1)} - \{P_{t+\Delta t}\}^{(i-1)} \quad (9)$$

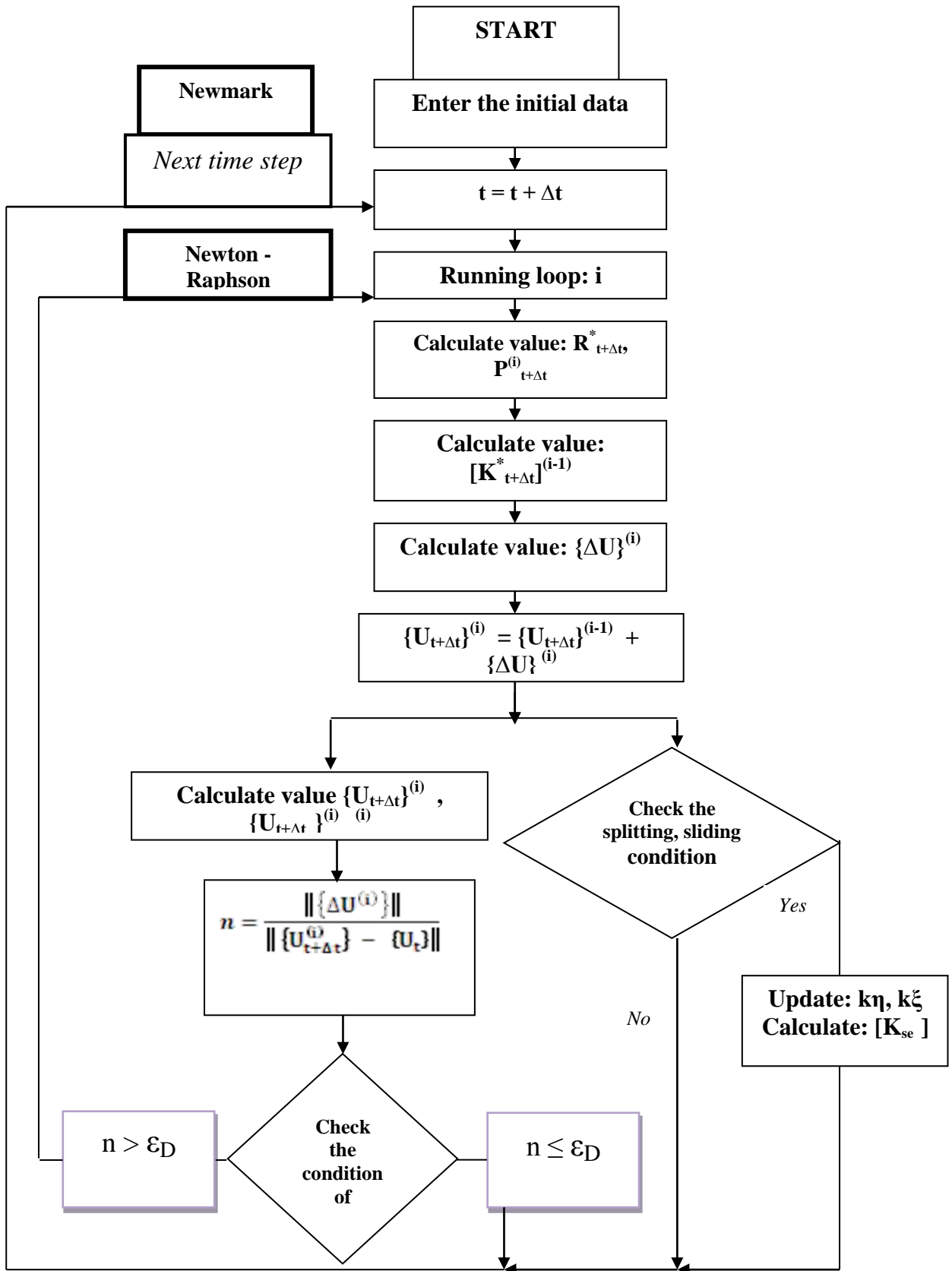


Figure 5. Flowchart of algorithm

in which:

$[K_{t+\Delta t}^*]^{(i-1)}$: is effective stiffness matrix (at the (i-1) time step).

$\{R_{t+\Delta t}^*\}^{(i-1)}$: is load vector (at the (i-1) time step).

$\{P_{t+\Delta t}\}^{(i-1)}$: is the internal force vector (at the (i-1) time step)

The initial value problem at the time step:

$$\{U_{t+\Delta t}\}^{(0)} = \{U_t\}; \{P_{t+\Delta t}\}^{(0)} = \{P_t\};$$

$$\{K_{t+\Delta t}\}^{(0)} = \{K_t\} \quad (10)$$

And for solving the nonlinear problems, we are using the process of iteration Newton-Raphson method. The convergence condition of the one iteration step is included as follows [Bath and Wilson, 1982, Zienkiewicz and Taylor, 1986, Fadeev, 1995]:

$$\frac{\|\{\Delta U\}^{(i)}\|}{\|\{U_{t+\Delta t}\}^{(i)} - \{U_{t+\Delta t}\}\|} \leq \varepsilon_D \quad (11)$$

where: ε_D is a user-defined tolerance number.

In every iteration step, depends on stress in contact element, checks the splitting, sliding condition between the pipe and substrate (accordance with standards Morh - Coulumb) and update value $k\eta$, $k\xi$ into the

stiffness matrix (contact element) [Amir Rahim, 1998, Nguyen, T. C., 2006].

Finite element method (FEM) algorithm diagram is described with details in Figure 5.

2.3. Numbering Example

Considering the conduit with inner diameter of $d = 1,6\text{m}$ and outer diameter of $D = 2\text{m}$ which lies in coral background with the depth of 4 meters, the elastic modulus of conduit material is $E_p = 210\text{ GPa}$, coefficients of Poisson $\nu_p = 0,3$ and density of $\rho_p = 7,8 \times 10^3 \text{ kg/m}^3$.

The background consists of four layers as specified in Figure 6 and physic – mechanical characteristics as specified in Table 3.

The conduit is under internal pressure of $p = 98,1\text{kPa}$, SXK load is evenly distributed over the surface with the rule as specified in Figure 7, effective loading time with $\tau = 0,05\text{s}$.

Choosing the calculations time with $t_{\text{cal}} = 15\tau$, margin error of researched domain boundary $\varepsilon = 0,5\%$ calculation error of $\varepsilon_D = 0,25\%$.

Figure 8 and Figure 9 show the corresponding displacement and nominal stress at point A (with and without p)

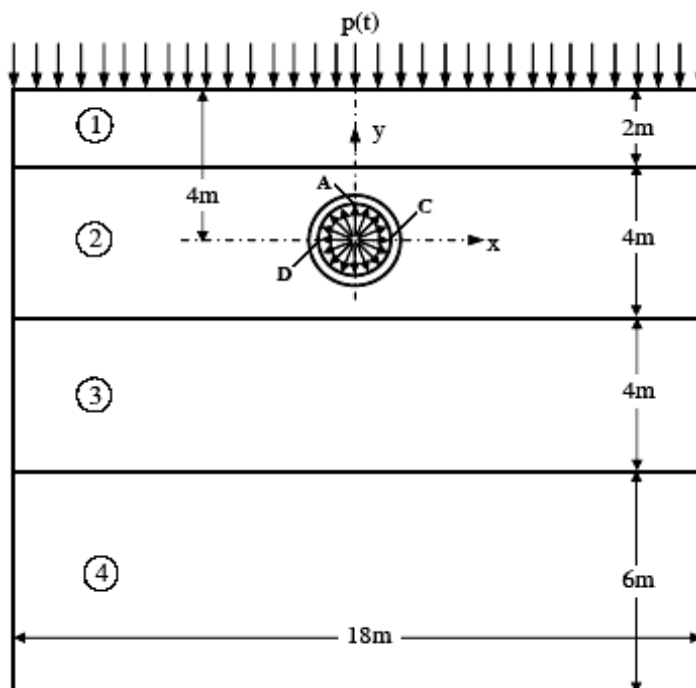


Figure 6. Model problem

$$\begin{cases} p(t) = p_m F(t), & p_m = 196.2\text{kPa} \\ F(t) = \begin{cases} 1 - \frac{t}{\tau} & 0 \leq t \leq \tau, \\ 0 & t > \tau \end{cases} \\ \tau = 0.05\text{s} \end{cases}$$

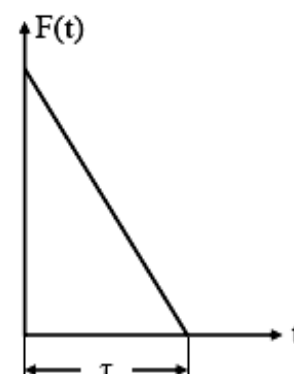
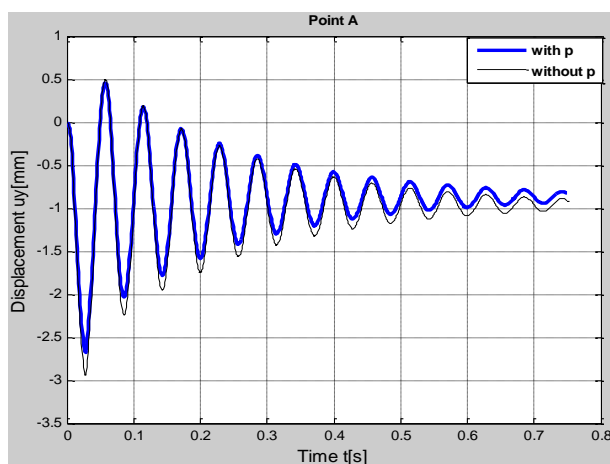
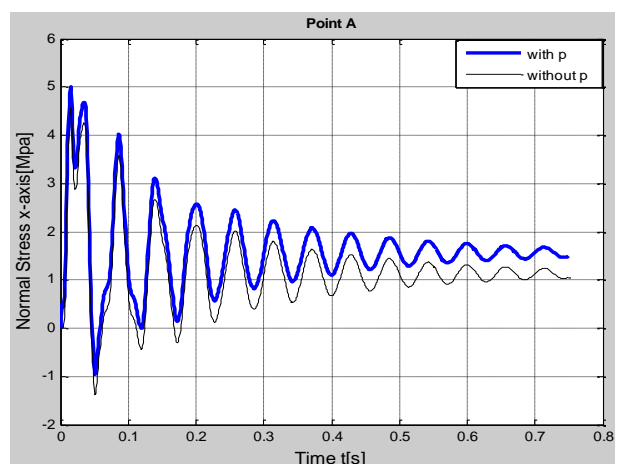


Figure 7. Load function

Table 3. Characterized coral substrate

Layer	Depth (m)	E_f (GPa)	ν_f	ρ_f (kg/m ³)	Friction coefficient f	The lead resistance ξ
1	2	0,28	0,22	$2,5 \times 10^3$	0,21	0,05
2	6	2,10	0,25	$2,8 \times 10^3$	0,32	
3	10	20,0	0,25	$2,9 \times 10^3$	0,41	
4	16	2,60	0,25	$2,0 \times 10^3$	0,47	

**Figure 8.** Displacement U_y at point A (with and without p)**Figure 9.** Normal stress σ_x at point A (with and without p)

2.4. Investigating the effect of some factors on stress, displacement of the pipe (with $p = 98,1 \text{ kPa}$)

2.4.1. The Influence of substrate layer around pipe

Survey of variation of E_f elastic modulus

Table 4

u_y^{\max} , σ_x^{\max} and E_f

E_f [GPa]	1,5	1,8	2,1	2,4	2,7	3,0	3,3	3,6
u_y^{\max} [mm]	2,8167	2,7375	2,6721	2,6241	2,5834	2,5479	2,5171	2,4930
σ_x^{\max} [MPa]	5,8021	5,3421	4,9944	4,6503	4,3761	4,1637	3,9980	3,8322

2.4.2. The influence of pipe's material

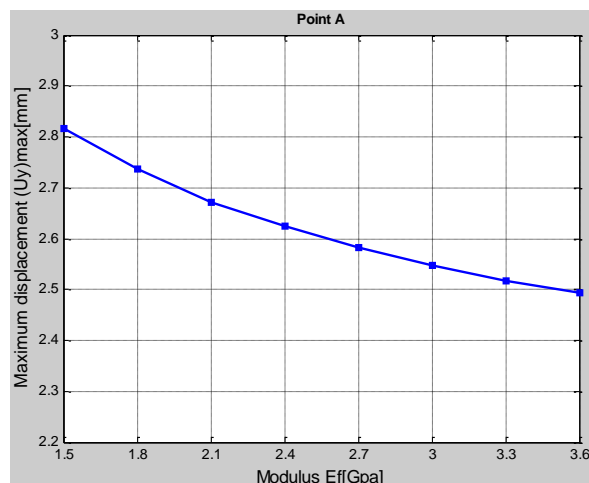
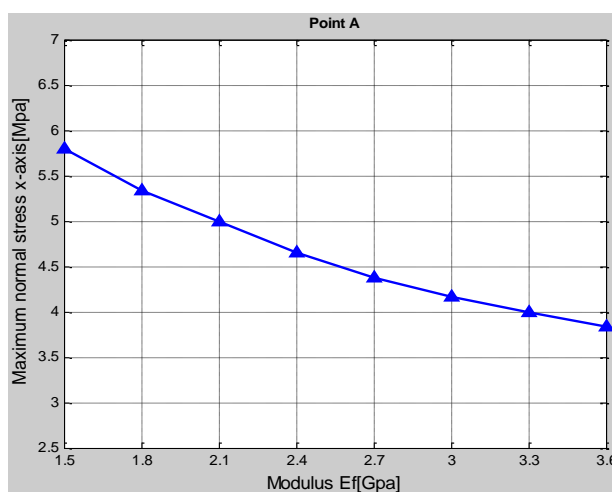
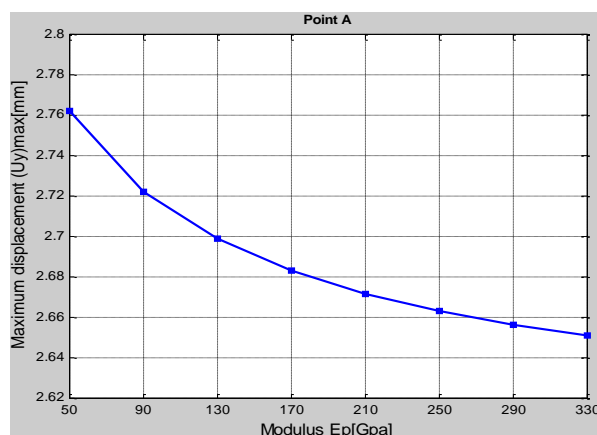
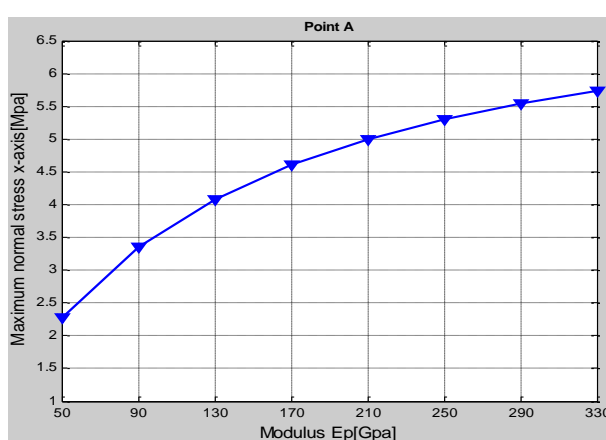
With elastic modulus of E_p conduit material is being various from 50GPa to 330GPa, the authors

with background layer that surrounds the conduit from 1,5GPa to 3,6GPa. And Table 4 and Figure 10 - Figure 11 show the changes of displacement and maximum stress at calculation point A of the conduit.

have identified the changes of displacement and maximum stress and at point A, as it can be seen in Table 5 and Figure 12 – Figure 13.

Table 5Variation of u_y^{\max} , σ_x^{\max} according to E_p

E_p [GPa]	50	90	130	170	210	250	290	330
u_y^{\max} [mm]	2,7625	2,7223	2,6991	2,6835	2,6721	2,6635	2,6566	2,6511
σ_x^{\max} [MPa]	2,2838	3,3588	4,0820	4,6026	4,9944	5,2986	5,5404	5,7366

**Figure 10.** Correlation of u_y^{\max} - E_f **Figure 11.** Correlation of σ_x^{\max} - E_f **Figure 12.** Correlation of u_y^{\max} - E_p **Figure 13.** Correlation of σ_x^{\max} - E_p

2.4.3. The influence of the substrate's surface

With elastic modulus E_f of the substrate 1 (layer 1) ranged from 0,5GPa to 2,6GPa. Results are shown in the Figures 14 and Figure 15.

Remarks

- In case of conduit not being under internal pressure: the maximum displacement

of u_y^{\max} at A increases 10.12%, stress of σ_x^{\max} Points A increases 8.67%.

- In case of the conduit being under internal pressure:

- When E_f modulus of background layer which surrounds the conduit increases from 1,5 GPa to 3,3 GPa then at point A, it shows

that: displacement of u_y^{\max} decreases 11,49% and stress σ_x^{\max} decreases 33,95%;

○ When E_p modulus of the conduit increases from 50 GPa to 330 GPa, then at point A of the conduit, it shows that: displacement of u_y^{\max} decreases 4,03% and

stress σ_x^{\max} increases 15,12%;

○ When E_f modulus of background layer of surface increases from 0,5 GPa đến 2,6 GPa, then at point A of the conduit, it shows that: displacement of u_y^{\max} decreases 24,43% and stress σ_x^{\max} decreases 34,06%.

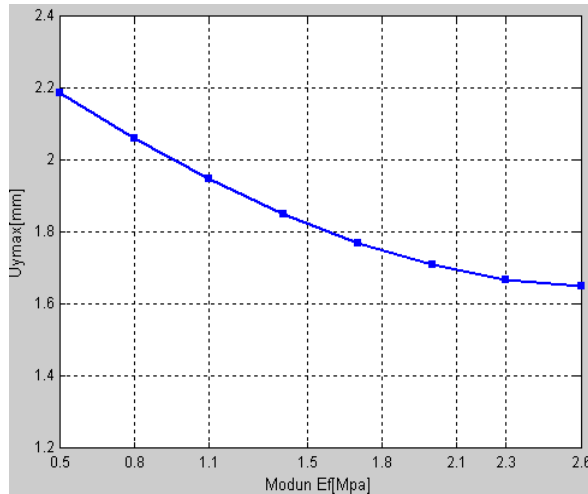


Figure 14. Correlation of u_y^{\max} - E_f

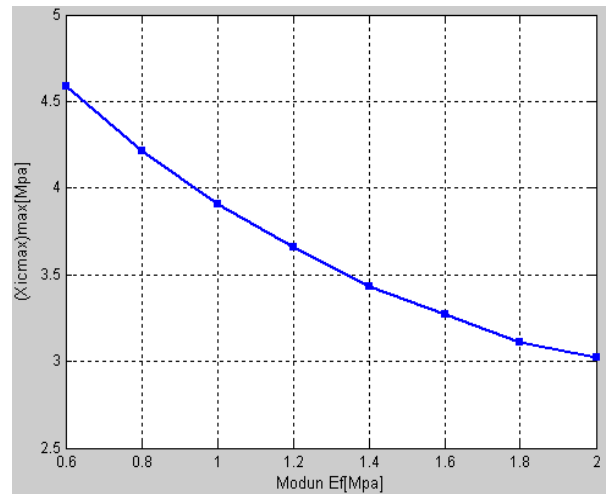


Figure 15. Correlation of σ_x^{\max} - E_f

3. Conclusions

The paper has achieved the following key results:

- Research and release the results of geological characteristics in depth (51,2m) of the coral foundation in Southwest Cay Islands - Spratly Islands;
- Conducting algorithms finite element

model and software programs solving interaction problem between pipe and coral foundation under the effect of shockwave loading capacity; conducting a survey of factors affecting stressor, displacement of the pipe allowing quantification assessment of the impact of these factors on the work of the pipeline■

References

- Amir Rahim (1998). *Joint Interface (Slip) Elements in Crisp in 2D and 3D Space*. Crisp-97 Development Report.
- Bath, K. J. and Wilson, E. L. (1982). *Numerical Method in Finite Element Analysis*. NJ: Prentice-Hall, Inc., Englewood Cliffs.
- Hoang, X. L. (2005) *Recapitulative report of the subject No KC.09.08*. Le Quy Don University.
- Nguyen, T. C. (2006). *Coral foundation and working of pile in coral foundation*, PhD Thesis, Le Quy Don University.
- Nguyen, T. C., Hoang, X. L., Pham, T. D., Le. T. (2008) Calculating dynamic interaction between the pipe and the coral foundation. *Proceeding of The National Conference on Computational Solid Mechanics*, 259-268.
- Zhu, F. and Lu, G. (2007). A Review of Blast and Impact of Metallic and Sandwich Structures. *EJSE Special Issue: Loading on Structures*, 92-101.
- Zienkiewicz, O. C. and Taylor, R. L. (1986). *The Finite Element Method: Solid mechanics*, NY: Mcgraw Hill Book Company.